33rd Annual International Conference of the IEEE EMBS
Boston, Massachusetts USA, August 30 - September 3, 2011

Polynomial Regularization for Robust MRI-based Estimation of Blood Flow Velocities and Pressure Gradients

Michael Delles, Fabian Rengier, Sebastian Ley, Hendrik von Tengg-Kobligk, Hans-Ulrich Kauczor, Rüdiger Dillmann, and Roland Unterhinninghofen

Abstract— **In cardiovascular diagnostics, phase-contrast MRI is a valuable technique for measuring blood flow velocities and computing blood pressure values. Unfortunately, both velocity and pressure data typically suffer from the strong image noise of velocity-encoded MRI. In the past, separate approaches of regularization with physical a-priori knowledge and data representation with continuous functions have been proposed to overcome these drawbacks. In this article, we investigate polynomial regularization as an exemplary specification of combining these two techniques. We perform time-resolved three-dimensional velocity measurements and pressure gradient computations on MRI acquisitions of steady flow in a physical phantom. Results based on the higher quality temporal mean data are used as a reference. Thereby, we investigate the performance of our approach of polynomial regularization, which reduces the root mean squared errors to the reference data by 45% for velocities and 60% for pressure gradients.**

I. INTRODUCTION

In management of cardiovascular diseases, information about blood flow velocities and blood pressures is of great importance. Since sphygmomanometry isn't able to deliver time-resolved blood pressure values for arbitrary vessels, pressure measurements by catheterization are commonly used. However, these methods suffer from their invasiveness, use of radiation and the lack of spatial information.

Images of the flow velocities inside the blood vessels can be obtained by techniques like phase-contrast magnetic resonance imaging (PC-MRI). In recent years, methods to compute pressure gradients and relative pressures from velocity-encoded MRI by using the momentum conservation of the Navier-Stokes equations have been developed.

Among others, notable work was done by Yang et al. [1], [2], Ebbers et al. [3], [4], Fatouraee and Wang et al. [5]-[11], Tyszka et al. [12], Balleux-Buyens et al. [13], Song et al. [14], Bolin et al. [15], Thompson et al.[16], Lum et al. [17] and Moftakhar et al. [18]. Non-invasive MRI-based blood pressure computation is very promising due to the possibility to obtain spatially resolved pressure values inside the vessels. However, since the blood flow velocity images are given as discrete voxel volumes, discretized Navier-Stokes equations have to be used. Together with the typically low spatio-temporal resolution and low signal-to-noise ratios of PC-MRI, numerical derivations in the discretized equations lead to an amplification of image noise. Thus, the accuracy of the blood pressure computations is limited. Furthermore, cumbersome iterative numerical integration schemes [3], [19] have to be applied to compute relative pressures from the noisy, discrete pressure gradients.

Several strategies to increase the robustness and accuracy of the blood pressure computation methods have been investigated. Regularization of the given discrete velocity images is proposed by Song et al. [5], [14] and Bolin et al. [15]. Jiraraksopakun et al. [20], [21] apply this technique to velocity measurements using Tagged-MRI. These regularization techniques incorporate physical a-priori knowledge to minimize the influence of noise and imaging artifacts in the underlying velocity images. This a-priori knowledge can e.g. be given by the incompressible form of the continuity equation, also known as the divergence-free condition. The fulfillment of the physical a-priori knowledge is normally achieved by minimizing an error function, which consists of the weighted sum of the distance to the measured velocity images and the distance to a perfect fulfillment of the physical a-priori knowledge. Thereby, adjusting the method by changing the weights inside the error function is possible. However, by still using the discrete velocity images, the degrading effects of applying discretized Navier-Stokes equations are still present.

On the other hand, continuous functions can be used to represent the blood flow velocity images [8], [22] or the pressure gradient data [10], [11]. Up to now, these techniques only incorporate physical a-priori knowledge as an implicit property of the basis functions. Skrinjar et al. [22] for instance use divergence-free radial basis functions. These techniques of continuous representation overcome the drawbacks of discretized Navier-Stokes equations. However, unlike the methods mentioned in the last paragraph, they lack the possibility of choosing the weighting between physical a-priori knowledge and measured data. This could possibly lead to solutions which differ too much from the original

M. Delles is with the Institute for Anthropomatics, Karlsruhe Institute of Technology (KIT), 76131 Karlsruhe, Germany. (email: delles@kit.edu)

F. Rengier is with the Department of Diagnostic and Interventional Radiology, University Hospital Heidelberg, 69120 Heidelberg, Germany and with the Department of Radiology E010, German Cancer Research Center (dkfz), 69120 Heidelberg, Germany.

S. Ley is with the Department of Diagnostic and Interventional Radiology, University Hospital Heidelberg, 69120 Heidelberg, Germany and with the Department of Medical Imaging, University of Toronto, M5S 1A1 Toronto, Ontario, Canada.

H. von Tengg-Kobligk is with the Department of Diagnostic and Interventional Radiology, University Hospital Heidelberg, 69120 Heidelberg, Germany and with the Department of Radiology E010, German Cancer Research Center (dkfz), 69120 Heidelberg, Germany.

H.-U. Kauczor is with the Department of Diagnostic and Interventional Radiology, University Hospital Heidelberg, 69120 Heidelberg, Germany.

R. Dillmann is with the Institute for Anthropomatics, Karlsruhe Institute of Technology (KIT), 76131 Karlsruhe, Germany.

R. Unterhinninghofen is with the Institute for Anthropomatics, Karlsruhe Institute of Technology (KIT), 76131 Karlsruhe, Germany.

978-1-4244-4122-8/11/$26.00 ©2011 IEEE

measurements in favor of completely fulfilled physical a-priori knowledge.

Therefore, we propose a method of combining both approaches by using regularization with arbitrarily weighted physical a-priori knowledge and representation using continuous functions. Thus, we want to achieve robust MRI-based blood flow velocity measurements and blood pressure gradient computations. In the present work, we investigate an exemplary specification of such a regularization model using continuous polynomial functions, the divergence-free condition as physical a-priori knowledge and a genetic algorithm for minimizing the error function. We use PC-MRI measurements of steady flow in a physical phantom to assess the influence of the polynomial order and of the weights inside the error function on the quality of velocity and pressure gradient data.

II. METHODS

A. Polynomial Regularization

We acquire three-dimensional, time-resolved images of three-directional flow velocity vectors using PC-MRI. The velocity images are given as discrete voxels (x, y, z) with velocity vectors $V(x, y, z) = (V_x(x, y, z), V_y(x, y, z), V_z(x, y, z))$. In order to minimize the influence of image noise and artifacts on the velocity data and the subsequent pressure gradient computation, we apply our approach of polynomial regularization. Each component of the discrete velocities V is represented by a continuous polynomial function $\hat{V}_x$, $\hat{V}_y$ and $\hat{V}_z$ of equal order o. The polynomial functions $\hat{V} = (\hat{V}_x, \hat{V}_y, \hat{V}_z)$ depend on unknown coefficients, which are computed by minimizing an error function

$$F = \lambda_1 f_1 + \lambda_2 f_2 \tag{1}$$

$$f_1 = \|\hat{V} - V\| \tag{2}$$

$$f_2 = \|\nabla \cdot \hat{V}\| \,. \tag{3}$$

The distance to the measured velocities V is represented by f_1. As physical a-priori knowledge, the divergence f_2 of the resulting polynomial functions is taken. This value is known to be zero for real incompressible flows. The weight factor $\lambda = \frac{\lambda_2}{\lambda_1}$ adjusts the weighting between the two parts of the error function. We minimized the error function using a genetic algorithm as proposed by Jiraraksopakun et al. [20], [21]. This iterative algorithm produces a set of possible solutions, mutates and combines them and selects the best solutions for the next iteration according to their fitness function. The initial values for the unknown polynomial coefficients were computed using QR-factorization. A population size of 20 possible solutions and a fixed number of 50 maximum iterations were used. All data analysis was performed in MATLAB (Mathworks, Inc.).

B. Pressure Gradient Computation from Velocity Images

If blood is modeled as an incompressible, Newtonian fluid and laminar flow is assumed, the momentum conservation of the Navier-Stokes equations is given by

$$G := \nabla p = -\rho \frac{\partial V}{\partial t} - \rho (V \cdot \nabla) V + \mu \nabla^2 V + b \,, \tag{4}$$

where the body forces b are normally neglected. Using the blood's density ρ and viscosity μ, the pressure gradient G can be computed from the velocities V. For the computation of pressure gradients from the discrete velocities V, we discretized (4) using central differences. In contrast, pressure gradients from the continuously represented velocities $\hat{V}$ were computed using (4) with analytical derivations.

C. Evaluation Using PC-MRI of a Physical Phantom

Using a standard clinical 1.5-T whole-body system (Avanto, Siemens, Erlangen, Germany) and a clinical time-resolved three-directional PC sequence (VENC=100 cm/s), we performed velocity-encoded MRI acquisitions of steady flow in a phantom [23] which mimics a stenotic human vessel. We measured 30 time frames with a temporal resolution of 32 ms. The velocity vectors in an image volume of 20x20x20 voxels with a reconstructed voxel size of 1.55x1.55x2.1 mm^3 covering the entry region of the stenosis were extracted. By this means, we obtained the velocity vectors V for one arbitrarily chosen time frame and the temporal mean $\bar{V}$ of the velocity vectors over all time frames. Using the discretized version of (4), we computed pressure gradient values G from the velocities V and $\bar{G}$ from the velocities $\bar{V}$. Furthermore, we computed the polynomial functions $\hat{V}$ from the given noisy velocity data V by applying our approach of polynomial regularization. Afterwards, we derived the pressure gradients $\hat{G}$ from $\hat{V}$ using the analytical version of (4).

Since the temporally averaged velocities suffer less from image noise, $\bar{V}$ and $\bar{G}$ are assumed to be of higher quality than V and G. Thus, we computed the error fraction $E_V = R(\hat{V})/R(V)$ using the root mean squared error $R(V)$ between V and $\bar{V}$ and the root mean squared error $R(\hat{V})$ between $\hat{V}$ and $\bar{V}$, in order to evaluate the performance of our approach. For the pressure gradients, an analog derivation of E_G was performed. For these computations, the continuously represented data $\hat{V}$ and $\hat{G}$ were sampled with the spatial resolution of the discrete fields V and G. An error fraction of $E_V < 1$ and $E_G < 1$ indicates an error reduction created by the use of polynomial regularization. As an additional quality criterion, we computed the root mean squared divergence d of the velocity fields V, $\bar{V}$ and $\hat{V}$. Since the divergence should be zero in an incompressible flow, lower values of d indicate higher quality of the velocity fields. We investigated the influence of the polynomial order o and the weight factor λ in the minimized error function ($o = \{4, 7, 10, 13\}, \lambda = \{0, 5, 10, 15\}$).

III. RESULTS

Fig. 1 shows the velocities on a central slice through the phantom, whose longitudinal axis is parallel to the y-direction. Fig. 1(a) depicts the velocity magnitudes $|V|$ of one time frame and Fig. 1(b) the mean velocity magnitudes $|\bar{V}|$ over all time frames. As expected, the velocity inside the stenosis (y=30mm) is increased compared to outside the stenosis (y=0mm) and generally declines towards the vessel wall (x=0mm, x=30mm). In the velocities $|\hat{V}|$ after polynomial regularization (o=13, λ=15), the errors caused by the image noise are reduced compared to $|V|$ (see Fig. 1(c)). The maximum difference to $|\bar{V}|$ decreases from 31.84 cm/s for $|V|$ to 17.43 cm/s for $|\hat{V}|$.

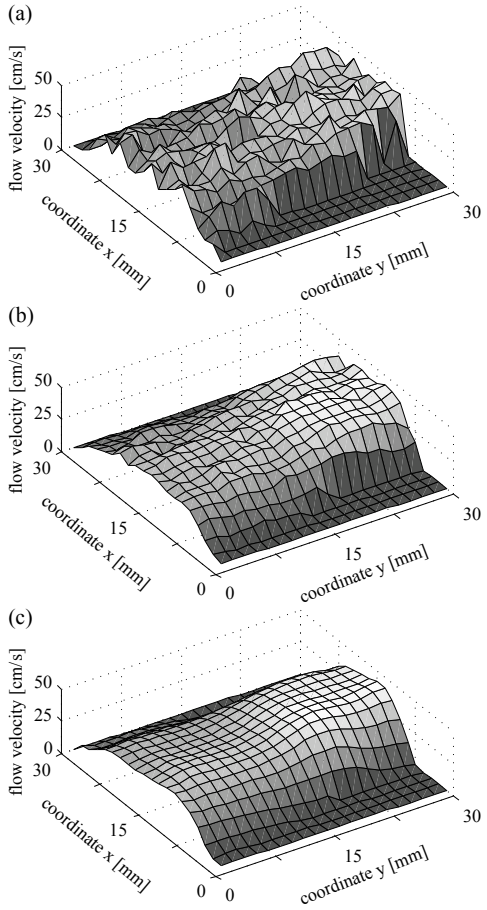

Fig. 1. Magnitude of flow velocity: (a) one time frame: $|V|$. (b) mean over all time frames: $|\bar{V}|$. (c) one time frame with polynomial regularization: $|\hat{V}|$.

The error fractions for different polynomial orders o and weight factors λ are depicted in Fig. 2. In every case, the error fractions E_V for the velocity and E_G for the pressure gradient are significantly smaller than 1, thereby showing that polynomial regularization decreased the errors caused by the noisy MRI data. The mean error fraction over all orders o and weight factors λ is E_V=0.55 and E_G=0.40, which corresponds to a reduction of the root mean squared errors by 45% and 60%. Thus, the improvement created by our approach is stronger in the pressure gradient than in the velocity data.

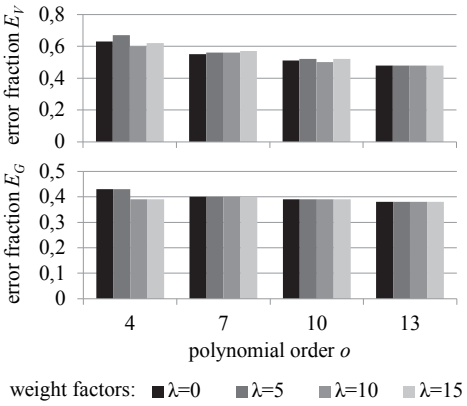

Fig. 2. Error fractions of velocity (E_V) and pressure gradient (E_G) after application of polynomial regularization.

The error fractions decrease with higher orders o and are only marginally influenced by the weight factors λ, whose impact on the divergence d of the resulting velocity fields $\hat{V}$ is shown in Table I. Smaller divergence values are achieved if higher weight factors are used. This effect is stronger in polynomials with lower orders. Furthermore, the divergence values are generally higher if higher orders o are used. All divergence values of $\hat{V}$ are significantly lower than the divergences without polynomial regularization (V: d=37.74 1/s, $\bar{V}$: d=13.95 1/s).

TABLE I
DIVERGENCE OF VELOCITY FIELDS

	o=4	**o=7**	**o=10**	**o=13**
λ=0	1.08 / 100%	2.59 / 100%	3.96 / 100%	6.03 / 100%
λ=5	0.49 / 45.4%	2.47 / 95.4%	3.92 / 99.0%	6.02 / 99.8%
λ=10	0.51 / 47.2%	2.43 / 93.8%	3.85 / 97.2%	5.95 / 98.7%
λ=15	0.47 / 43.5%	2.42 / 93.4%	3.87 / 97.7%	5.94 / 98.5%

Root mean squared divergence of the velocity field $\hat{V}$. Values are shown in [1/s] and in percentage of the corresponding values with λ=0.

Fig. 3 shows the pressure gradient magnitudes along the vessel axis. As expected, the data $|G|$ shows higher image noise than $|\bar{G}|$. Applying polynomial regularization (o=13, λ=15) minimizes the influence of noise in $|\hat{G}|$ and decreases the maximum difference to $|\bar{G}|$ along the vessel axis from 1.597 mmHg/m for $|G|$ to 0.391 mmHg/m for $|\hat{G}|$.

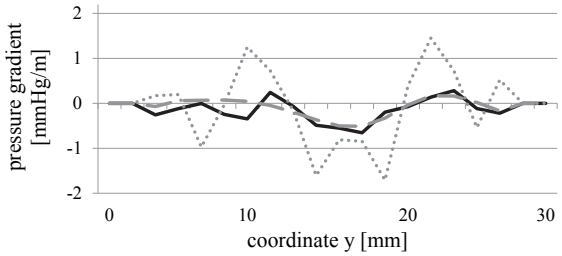

Fig. 3. Magnitude of the axial pressure gradient along the vessel axis: mean over all time frames ($|\bar{G}|$, solid), one time frame without ($|G|$, dotted) and with ($|\hat{G}|$, dashed) polynomial regularization.

IV. DISCUSSION

As expected, the measured velocities and derived pressure gradients of one time frame of the MRI acquisition of the physical phantom show stronger errors than the temporal mean of all time frames. These errors were decreased in all performed experiments by applying our approach of polynomial regularization. Higher polynomial orders o lead to smaller errors concerning the error fractions E_V and E_G, but they increase the divergence d of the resulting velocity field. Therefore, a trade-off between these quality criteria concerning the choice of the polynomial order has to be addressed. Higher weight factors λ further decrease the divergence d. This effect is less visible for higher orders o, possibly related to the fixed number of iterations used for the genetic algorithm. Therefore, we plan to perform further investigations concerning this issue.

Overall, the presented evaluations show the general applicability of our approach of polynomial regularization. In the future, we want to perform further tests using MRI data of patients and healthy volunteers. Extending the theory of our approach to pulsatile flow is straight forward, but increases the computation times and could necessitate faster implementations. Furthermore, our presented investigations only form preliminary results for one exemplary specification of combining regularization and representation using continuous functions. We plan to investigate trigonometric, exponential or radial basis functions and additional criteria for the physical a-priori knowledge such as similar flow through adjacent vessel cross sections and no flow through the vessel wall. Thereby we want to further investigate if approaches of combining regularization with arbitrarily weighted physical a-priori knowledge and representation with continuous functions are successful in improving the accuracy of MRI-based blood flow velocity measurements and blood pressure gradient computations under realistic conditions.

REFERENCES

[1] G. Yang, P. Kilner, N. Wood, S. Underwood, and D. Firmin, "Computation of flow pressure fields from magnetic resonance velocity mapping," *Magnetic resonance in medicine*, vol. 36, no. 4, pp. 520-6, 1996.

[2] G. Yang, R. Merrifield, S. Masood, and P. Kilner, "Flow and myocardial interaction: an imaging perspective," *Philosophical Transactions of the Royal Society B: Biological Sciences*, vol. 362, no. 1484, p. 1329, 2007.

[3] T. Ebbers and G. Farnebäck, "Improving computation of cardiovascular relative pressure fields from velocity MRI," *Journal of Magnetic Resonance Imaging*, vol. 30, no. 1, pp. 54-61, 2009.

[4] T. Ebbers, L. Wigström, A. Bolger, B. Wranne, and M. Karlsson, "Noninvasive Measurement of Time-Varying Three-Dimensional Relative Pressure Fields Within the Human Heart," *Journal of Biomechanical Engineering*, vol. 124, p. 288, 2002.

[5] N. Fatouraee and A. Amini, "Regularization of flow streamlines in multislice phase-contrast MR imaging," *IEEE Transactions on Medical Imaging*, vol. 22, no. 6, pp. 699-709, 2003.

[6] A. Moghaddam, E. Choi, and A. Amini, "Fast computation of static flow pressure maps from phase-contrast MRI in axi-symmetric coordinates," *Proceedings of the Second Joint EMBS/BMES Conference*, vol. 2, pp. 931-932, 2002.

[7] A. Nasiraei-Moghaddam, G. Behrens, N. Fatouraee, R. Agarwal, E. Choi, and A. Amini, "Factors affecting the accuracy of pressure measurements in vascular stenoses from phase-contrast MRI," *Magnetic Resonance in Medicine*, vol. 52, no. 2, pp. 300-309, 2004.

[8] A. Pashaee, G. Ataee, M. Rezazadeh, and N. Fatouraee, "One-dimensional evaluation of a least-square polynomial fitting approach to estimate the pressure domain from velocity data obtained from medical images," *3rd Kuala Lumpur International Conference on Biomedical Engineering 2006*, Springer, pp. 278-281, 2007.

[9] A. Pashaee, P. Shooshtari, G. Ataei, and N. Fatouraee, "The Role of Velocity Map Quality in Estimation of Intravascular Pressure Distribution, Proceedings of World Academy of Science," *Engineering and Technology*, vol. 11, pp. 271-276, 2006.

[10] Y. Wang and A. Amini, "Integrable Pressure Gradients via Harmonics-Based Orthogonal Projection," *Information Processing in Medical Imaging*, Springer, pp. 431-442, 2005.

[11] Y. Wang, A. Moghaddam, G. Behrens, N. Fatouraee, J. Cebral, E. Choi, and A. Amini, "Pulsatile pressure measurements via harmonics-based orthogonal projection of noisy pressure gradients," *Proc. SPIE Medical Imaging*, vol. 6143, p. 61430C, 2006.

[12] J. Tyszka, D. Laidlaw, J. Asa, and J. Silverman, "Three-Dimensional, Time-Resolved (4D) Relative Pressure Mapping Using Magnetic Resonance Imaging," *Journal of Magnetic Resonance Imaging*, vol. 12, no. 2, pp. 321-329, 2000.

[13] F. Balleux, O. Jolivet, A. De Cesare, A. Herment, J. Tasu, and E. Mousseaux, "Estimation of the Diastolic Intraventricular Relative Pressures Using MRI Acceleration Measurements," *Lecture Notes in Computer Science*, vol. 2674, pp. 262-271, 2003.

[14] S. Song, R. Leahy, D. Boyd, B. Brundage, and S. Napel, "Determining cardiac velocity fields and intraventricular pressure distribution from a sequence of ultrafast CT cardiac images," *IEEE Transactions on Medical Imaging*, vol. 13, no. 2, pp. 386-397, 1994.

[15] C. Bolin and L. Raguin, "Methodology to estimate the relative pressure field from noisy experimental velocity data," *Journal of Physics: Conference Series*, vol. 135, p. 012020, 2008.

[16] Thompson and E McVeigh, "Fast measurement of intracardiac pressure differences with 2D breath-hold phase-contrast MRI," *Magnetic Resonance in Medicine*, vol. 49, no. 6, pp. 1056-1066, 2003.

[17] D. Lum, K. Johnson, R. Paul, A. Turk, D. Consigny, J. Grinde, C. Mistretta, and T. Grist, "Transstenotic Pressure Gradients: Measurement in Swine - Retrospectively ECG-gated 3D Phase-Contrast MR Angiography versus Endovascular Pressure-sensing Guidewires," *Radiology*, vol. 245, no. 3, p. 751, 2007.

[18] R. Moftakhar, B. Aagaard-Kienitz, K. Johnson, P. Turski, A. Turk, D. Niemann, D. Consigny, J. Grinde, O. Wieben, and C. Mistretta, "Noninvasive measurement of intra-aneurysmal pressure and flow pattern using phase contrast with vastly undersampled isotropic projection imaging," *American Journal of Neuroradiology*, vol. 28, no. 9, p. 1710, 2007.

[19] G. Farnebäck, J. Rydell, T. Ebbers, M. Andersson, and H. Knutsson, "Efficient Computation of the Inverse Gradient on Irregular Domains," *IEEE 11th International Conference on Computer Vision (ICCV)*, pp. 1-8, 2007.

[20] Y. Jiraraksopakun, M. McDougall, S. Wright, and J. Ji, "A regularized flow quantification method using MRI tagging and Single Echo Acquisition imaging," *30th Annual International IEEE EMBS Conference*, pp. 3397 -3400, 2008.

[21] Y. Jiraraksopakun, M. McDougall, S. Wright, and J. Ji, "A Flow Quantification Method Using Fluid Dynamics Regularization and MR Tagging," *IEEE Transactions on Biomedical Imaging*, vol. 57, pp. 1437-1445, 2010.

[22] O. Skrinjar, A. Bistoquet, J. Oshinski, K. Sundareswaran, D. Frakes, and A. Yoganathan, "A divergence-free vector field model for imaging applications," *Proceedings of the Sixth IEEE international conference on Symposium on Biomedical Imaging: From Nano to Macro. IEEE Press*, pp. 891-894, 2009.

[23] M. Delles, F. Rengier, S. Ley, H. von Tengg-Kobligk, H.-U. Kauczor, R. Unterhinninghofen, and R. Dillmann, "Influence of imaging quality on magnetic resonance-based pressure gradient measurements," *Proc. SPIE Medical Imaging*, vol. 7626, p. 762624, 2010.